Oil Spill Detection and Visualization from UAV Images using Convolutional Neural Networks

Valério N. Rodrigues Junior[1], Roberto J. M. Cavalcante[1], João A. G. R. Almeida[1], Tiago P. M. Fé[1],
Ana C. M. Malhado[2], Thales Vieira[1][a] and Krerley Oliveira[3][b]

[1]*Institute of Computing, Federal University of Alagoas, Maceió, AL, Brazil*
[2]*Institute of Biological and Health Sciences, Federal University of Alagoas, Maceió, AL, Brazil*
[3]*Institute of Mathematics, Federal University of Alagoas, Maceió, AL, Brazil*

Keywords: Oil Spill, Convolutional Neural Network, Deep Learning, Ummanned Aerial Vehicles, Geospatial Data Analysis.

Abstract: Marine oil spills may have devastating consequences for the environment, the economy, and society. The 2019 oil spill crisis along the northeast Brazilian coast required immediate actions to control and mitigate the impacts of the pollution. In this paper, we propose an approach based on Deep Learning to efficiently inspect beaches and assist response teams using UAV imagery through an inexpensive visual system. Images collected by UAVs through an aerial survey are split and evaluated by a Convolutional Neural Network. The results are then integrated into heatmaps, which are exploited to perform geospatial visual analysis. Experiments were carried out to validate and evaluate the classifiers, achieving an accuracy of up to 93.6% and an F1 score of 78.6% for the top trained models. We also describe a case study to demonstrate that our approach can be used in real-world situations.

1 INTRODUCTION

Marine oil spills are one of the highest profiles and ecologically destructive polluting events with social and environmental consequences that can last many years after the oil has been removed/dispersed (Burger, 1997; Kingston, 2002).

For instance, the highly publicized 1989 spill of oil from the Exxon Valdez into Prince William Sound, Alaska was initially responsible for an enormous increase in mortality followed by prolonged sub-lethal effects that have led to the postponed recovery of many species (Peterson et al., 2003). Likewise, a recent review of the 2010 Deepwater Horizon oil spill in the northern Gulf of Mexico (Beyer et al., 2016) revealed a multiplicity of biological effects, with long-term impacts on large fish species, deep-sea corals, sea turtles, and cetaceans. Both the Exxon Valdez and Deepwater Horizon spills had a clear point of origin in time and space, with scientists able to closely monitor the spread of oil and the consequences of the pollution very soon after the spill had occurred.

[a] https://orcid.org/0000-0001-7775-5258
[b] https://orcid.org/0000-0002-7385-3114

This is very different from the recent (and still mysterious) oil spill in Brazil whose origin and timing are still unclear despite intensive investigation (Magris and Giarrizzo, 2020; Zacharias et al., 2021). The first indication that a major oil spill had occurred off the northeast coast of Brazil was the presence of large quantities of oil on beaches in August/September 2019 (Soares et al., 2020). Up to March 2020 reports of oiled areas were recorded in nearly 550 sites spanning 3000 km of coastline, affecting up to 55 environmental protection areas (Ladle et al., 2020). A study in Alagoas State indicates that fish and seafood sales decreased by more than 50% strongly impacting some of the most economically vulnerable communities of the northeast region. Likewise, tourism in the area was also dramatically affected (Ribeiro et al., 2021). Preliminary data suggests that diverse ecosystems were affected, including seagrasses (Magalhães et al., 2021), unique rhodolith beds (Sissini et al., 2020) and reef-building corals (Miranda et al., 2020). Soares *et al.* (Soares et al., 2020) identify four characteristics that make this oil spill unique: 1) the characteristics of the oil spill; 2) the characteristics of the affected region in tropical Brazil; 3) the scale of the disaster and; 4) the absence of measures and/or

flaws in the measures taken by the federal government to address this environmental and social emergency.

One of the major challenges in the early stage of such a disaster is to quickly collect accurate spatiotemporal oil pollution data (Soares et al., 2020). In this sense, Deep Learning (DL) approaches have achieved outstanding results in object detection and localization tasks during the last years (Redmon et al., 2016; Ren et al., 2016; Massa et al., 2021). Specifically, geospatial data analysis has greatly benefited from Deep Learning algorithms to tasks such as crop type detection (Kussul et al., 2017) and road extraction (Zhang et al., 2018), for instance. SAR remote sensing has been proposed for microplastic pollution in oceans (Davaasuren et al., 2018) and for marine oil spill detection (Shaban et al., 2021). In particular, the latter study is focused on segmenting large oil spills offshore using satellite images. In this work, we tackle a different problem: detecting and localizing tiny oil spills that may be washing up on beaches or inshore, using low cost unmanned aerial vehicles (UAV's).

A recent review (Fingas and Brown, 2018) claimed that oil spill detection using the visible spectrum is challenging, limiting the use of UAV's to perform such a task. More recently, Jiao *et al.* (Jiao et al., 2019) proposed a DL method to inspect facilities using UAV imagery, based on the Faster R-CNN (Ren et al., 2016). However, in that work oil spills' appearance, size and backgrounds are significantly different than in the problem we address herein. Consequently, we consider it a substantially different Computer Vision problem. We refer the reader to (Cazzato et al., 2020) for a comprehensive presentation on computer vision methods for UAV object detection.

In this paper, we propose a DL approach to assist response teams in the cleaning of oil spills washing up on beaches. In this situation, oil is usually scattered in many small connected compounds, which are found in a diversity of different backgrounds (sand, water, seaweed,...), as shown in Figures 1 and 5b. We exploit images acquired by low-cost UAVs to perform oil detection through an automated image analysis technique based on DL, achieving up to 93.6% of accuracy and an F_1 score of 78.6%. We also validate and evaluate our approach through a visual system that combines satellite imagery and heatmaps of oil density, to promptly and accurately notify response teams, thus avoiding significant environmental impacts.

The core of our approach is a Convolutional Neural Network (CNN) classifier, whose architecture was optimized to accurately recognize oil in small patches. Differently from more advanced deep neural network architectures, we opt for a small architecture specially trained to identify small oil spills in coastal land covers (*i.e.*, floating on the water surface or washing up on beaches). To integrate numerous CNN predictions in a visual manner, we propose a practical method to promptly and accurately notify response teams, thus avoiding significant environmental impacts.

Overall, our main contribution is to investigate whether a low-cost DL classifier, jointly with a visual interface, may provide quick, accurate and intuitive georeferenced information about small oil spills located on the beach or inshore, for rapid response purposes. In particular, the whole approach relies only on an inexpensive UAV and on a small neural network architecture, which is trainable in a low-cost desktop computer.

2 METHODOLOGY

Our approach is based on georeferenced RGB images collected through an aerial survey, by using UAVs. As illustrated in Figure 1, each image is first split into a grid of small patches. In the training phase, patches are manually annotated with a binary label indicating the presence of oil. Next, the supervised dataset is exploited to train a CNN binary classifier, which is then expected to recognize oil from small patches. In the detection phase, UAV images acquired through an aerial survey are first split into patches that are evaluated by the CNN. The resulting predictions are organized in oil maps representing the occurrence of oil in the region covered by each particular UAV image. The oil maps are combined with the original UAV images geolocations to build a heatmap (Nogueira et al., 2019) of the region covered in the aerial survey. Finally, the heatmap is superimposed over satellite imagery.

2.1 Imagery Acquisition, Preprocessing and Annotation

Firstly, a UAV collects georeferenced RGB imagery covering a region of interest, where oil may be potentially found. Each collected image covers a region that may contain superficial oil only in small subareas. Thus, to provide precise locations of oil spills, we propose to first split the captured images into small squared patches before training a CNN classifier capable of providing patch-level oil spills detections.

To train the CNN binary classifier, a dataset comprised of many of the aforementioned patches must be annotated by human trainers, in a binary fashion.
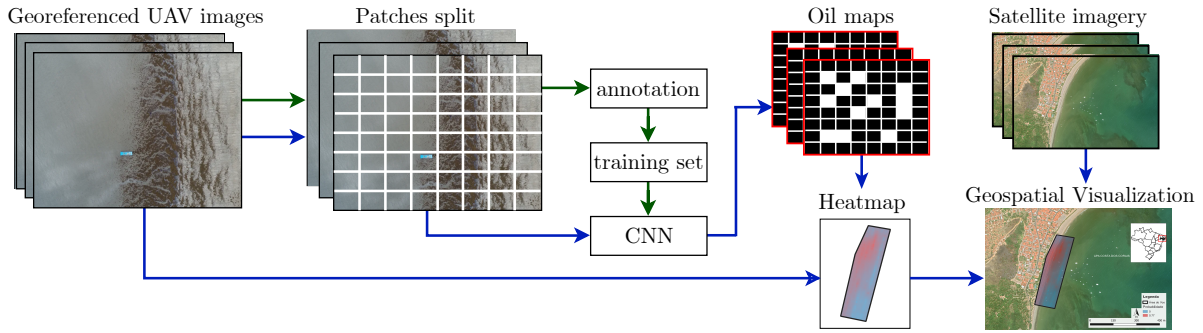
Figure 1: Overview of our approach, with two distinct phases: training a CNN classifier from small RGB patches (green arrows); and recognizing, localizing, and visualizing oil spots (blue arrows). As a common preprocessing step to both phases, UAV's georeferenced RGB imagery, acquired through an aerial survey, is split into small RGB patches.

In our experiments, we empirically concluded that this may be accomplished visually, without relying on prior oil spill geospatial information.

An appropriate patch size must satisfy both human trainers, who must be capable of visually recognizing oil in the patches; and the CNN classifier. In our experiments, we empirically found that a CNN could still achieve top results when each input patch was set to 128×128 pixels. This patch size was also satisfactory for the human annotation task. More specifically, we collected UAV images with spatial dimensions of 4864×3648 pixels, which were split into 1064 patches with a size of 128×128 pixels. A thorough investigation of optimal patch size parameters may be conducted in future work.

2.2 Supervised Classification

We adopt a classical CNN architecture but performed many experiments to tune hyperparameters. The input patches are first filtered by C blocks of convolutional layers with F filters of size K, followed by max-pooling layers. Then, the resulting feature maps are flattened and given as input to one or two dense layers with D_1 and D_2 units each. The output layer is made up of a single neuron with a sigmoid activation function, which outputs the probability of oil occurrence in the input patch. The hyperparameter search space is shown in Table 1 and the best classifier found in our experiments is revealed in Figure 2. More details on our experiments on hyperparameter optimization will be given in Section 3.

2.3 Postprocessing and Visual Geospatial Analysis

We propose to visually analyze the oil spill distribution in a specific area by computing heatmaps that integrate the outputs of the CNN classifier, and the geo-

coordinates of the images. Let I be an image, which is split into a grid $\mathcal{G}_I$ with $m \times n$ patches; and let $f_I[i, j] \in \{0, 1\}$ be the binary CNN prediction of the patch at the position $[i, j]$ of $\mathcal{G}_I$. Note that f_I is the *oil map* of image I, as shown in Figure 1. We define the density of oil in I, as the mean value of the oil map:

$$d_I = \frac{1}{m \cdot n} \sum_{i=1}^{m} \sum_{j=1}^{n} f_I[i, j]. \qquad (1)$$

By combining information from many images collected to cover a specific area of interest, we build a polygonal heatmap by interpolating the densities d_I using the geocoordinates g_I of image I. To this aim, we adopt the well-known Inverse Distance Weighting (IDW). Finally, to perform visual geospatial analysis, we employed the QGIS[1] system to plot the resulting heatmap over satellite imagery of the area of interest.

3 EXPERIMENTS

We performed experiments to validate the whole approach, compare and optimize CNN hyperparameters, and evaluate the best model performance. We also present a case study to investigate whether the proposed visual analysis system is appropriate to easily reveal oil pollution patterns in the images.

With this aim, we collected a dataset from *APA Costa dos Corais* – a coastal marine conservation unit

Table 1: Hyperparameter search space.

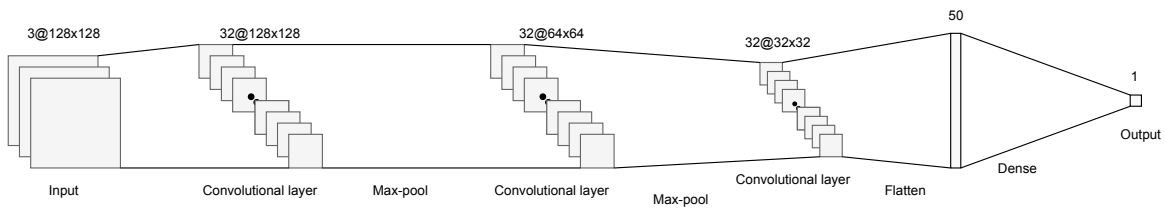| hyperparameter	values
C	1, 2 or 3
F	16, 32 or 64
K	3 or 5
D_1	25, 50 or 100
D_2	0, 25, 50 or 100

[1]https://qgis.org

Figure 2: Architecture of the top performing CNN.

located in the Brazilian states of Alagoas and Pernambuco. More specifically, data collection was carried out in the municipality of Japaratinga, Alagoas, in the peak phase of the crisis. A DJI Phantom 4 Advanced drone and the Dronedeploy[2] tool were used. Four flights were made, all at 60 meters high, collecting vertical images with a resolution of 1.8 centimeters per pixel and no filter. On average, each flight took 11 minutes and covered an area of roughly $70,000m^2$, resulting in approximately 200 images. The paths of the flights were planned to cover different types of areas including sand, seaweed, trees, seawater, and river water. Each flight covered a disjoint region of interest. Optimal flight hyperparameters, such as flight altitude, may be a topic of future research.

Some of the captured UAV images were manually chosen to compile a training set. Visual diversity was considered the main selection criterion, to assure that all types of covered areas were significantly represented. To avoid erroneous annotations, annotation redundancy (Puttemans et al., 2018) was adopted: each patch was annotated by at least two humans, and inconsistent annotations were then revised by a third human annotator. The final training set was comprised of 6,907 patches, which was split into 5,180 negative samples (not containing oil) and 1,727 positive samples (containing oil).

3.1 CNN Validation and Hyper-parameters Optimization

We performed a grid search over the hyperparameter search space described in Section 2.2 and summarized in Table 1. All possible combinations were experimented with through a cross-validation procedure by randomly splitting the dataset examples into training and test sets, considering 75% of the patches for training and 25% for testing, in a stratified manner. This procedure was repeated 10 times, and the average value was considered.

To train the networks, we adopted the Adam optimization algorithm (Kingma and Ba, 2014) of the Keras library (Chollet et al., 2015), which was employed to minimize the well-known categorical cross-

[2]https://www.dronedeploy.com

entropy loss with an initial learning rate of 0.001. Class imbalance of the dataset was tackled by setting each class weight to be inversely proportional to their respective frequency. However, since false negatives (patch containing oil, but not detected) are considered more harmful than false positive results (patch does not contain oil, but oil was detected) in this problem, the positive class weight was doubled. To put it another way, a false alarm would result in wasting response personnel resources. Missing oil spills, however, is much more harmful, due to environmental impacts.

Table 2 reveals the top 10 architectures, according to their F_1 score. One can see promising results, with many models achieving up to 93.59% of accuracy and an F_1 score of 78.6%. By visually examining some incorrectly predicted images shown in Figure 3, we found challenging and unusual situations, including very small oil spills hidden in seaweed; oil spills, resembling shadows in the water; a person using a black t-shirt, which looks similar to oil; and seaweed mixed with small black dots, which is similar to previously labeled small oil spills.

We also infer that, fortunately, the CNNs are not much sensitive to hyperparameters values in terms of accuracy: all top-performing networks achieved similar accuracy, even though their number of trainable weights varies greatly.

Nevertheless, this finding does not hold for the F_1 score, precision and recall, which are more suitable measures since the dataset is imbalanced. Furthermore, a high recall is more relevant than a high pre-
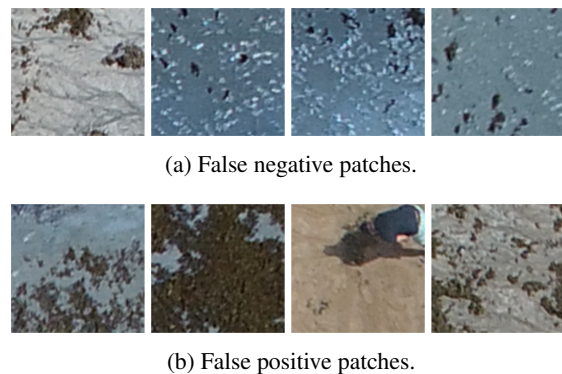

(a) False negative patches.

(b) False positive patches.

Figure 3: Examples of incorrect predictions.

Table 2: Configuration, F_1 score, accuracy, precision, recall and number of trainable weights of the top 10 CNN configurations and the compared methods, sorted by F_1 score. Best results in bold.

C	F	K	D_1	D_2	F_1 (%)	acc. (%)	prec. (%)	rec. (%)	weights
3	32	3	50	0	**78.6**	**93.6**	84.9	73.3	333,144
3	32	3	50	50	77.7	92.6	75.4	**80.1**	335,694
3	64	3	100	0	77.3	92.6	76.2	78.4	1,330,350
3	16	3	25	0	77.2	93.5	88.9	68.2	**83,565**
2	32	3	25	25	75.7	92.3	77.0	74.4	730,871
3	16	3	50	0	75.1	92.8	84.4	67.6	162,040
2	32	3	100	50	74.9	92.0	76.0	73.9	2,895,396
3	64	3	50	25	74.8	92.6	82.7	68.2	704,225
3	64	3	50	0	72.7	92.8	**92.9**	56.6	703,000
3	64	3	100	50	67.4	91.8	94.8	52.3	1,335,300
thresholding					56.9	71.0	48.2	69.6	-
HOG+SVM					22.0	72.0	24.0	20.0	-

cision, as aforementioned. The F_1 score of the top CNNs ranges from 67.4% to 78.6%, revealing high variance. This mostly occurred due to changes in the precision-recall tradeoff. Overall, we consider the second-best model to be an appropriate choice, since it achieved a recall of 80.1%, while still keeping a high accuracy of 92.6%. Besides, it is a small network with only 335,694 trainable weights. It is also worth considering that oil spills rarely occur in a single patch of the UAV image. Thus, a single UAV image comprised of several patches with oil spills will have its density of oil (Equation 1) underestimated by only approximately 20%, if the second-best model is used.

In summary, the presented results validate our machine learning approach and indicate that it may be effectively employed in real-world scenarios. As an alternative to avoid the costs related to false positive predictions, we suggest developing a more sophisticated visual interface where a human would visually validate reddish spots, before sending a response team.

3.2 Comparison with Baseline Image Classification Methods

We compare the results of our CNN classifiers to the traditional HOG+SVM (Han et al., 2006) approach, which combines Histogram of Gradients features with a linear Support Vector Machines (SVM) classifier; and to a baseline thresholding method (Vyas et al., 2015), since thresholding is a common oil spill detection approach (Al-Ruzouq et al., 2020). Class weighting was similarly employed for the compared methods, as described in Section 3.1. The results shown in Table 2 reveal inferior results for the HOG+SVM

method, with a poor F_1 score of 22%. Thresholding achieved intermediate results, with an F_1 score of 56.9% but still inferior to the top 10 CNN configurations. In this latter method, it is also worth noting a reasonable recall of 69.6%, which may be exploited in future work to improve the results of the CNN.

3.3 Case Study

In this case study, we followed the discussion of Section 3.1 and opted for the second-best model of Table 2, since it achieves the higher recall while keeping high accuracy and a small number of trainable weights, thus resulting in an accurate and computationally efficient model. The selected model was employed to predict all patches in a large area of $70,000m^2$ composed of 200 images collected by a drone flying over Japaratinga. Prediction time was approximately only 3 secs in a 2.5Ghz Intel i5 CPU with 8GB of RAM, since patches prediction occurred in batches.

After applying the postprocessing steps described in Section 2.3, the heatmap shown in Figure 4 was obtained. One can see the flight area bounded by a black polygon, with color-coded oil densities. The heatmap reveals a red spot in the northern part of the polygon, indicating a concentration of oil in that region that should be cleaned. It is worth noting that the location of this specific flight was chosen because of high concentrations of oil spills that were localized approximately in the reddish spots of Figure 4. This is qualitative evidence that validates our method. Figure 5 exhibit examples of a variety of correct predictions, including challenging situations in the sand, water, and seaweed. We thus conclude that the whole proposed approach is practical to rapidly identify oil pollution in beaches and allow a prompt response, minimizing
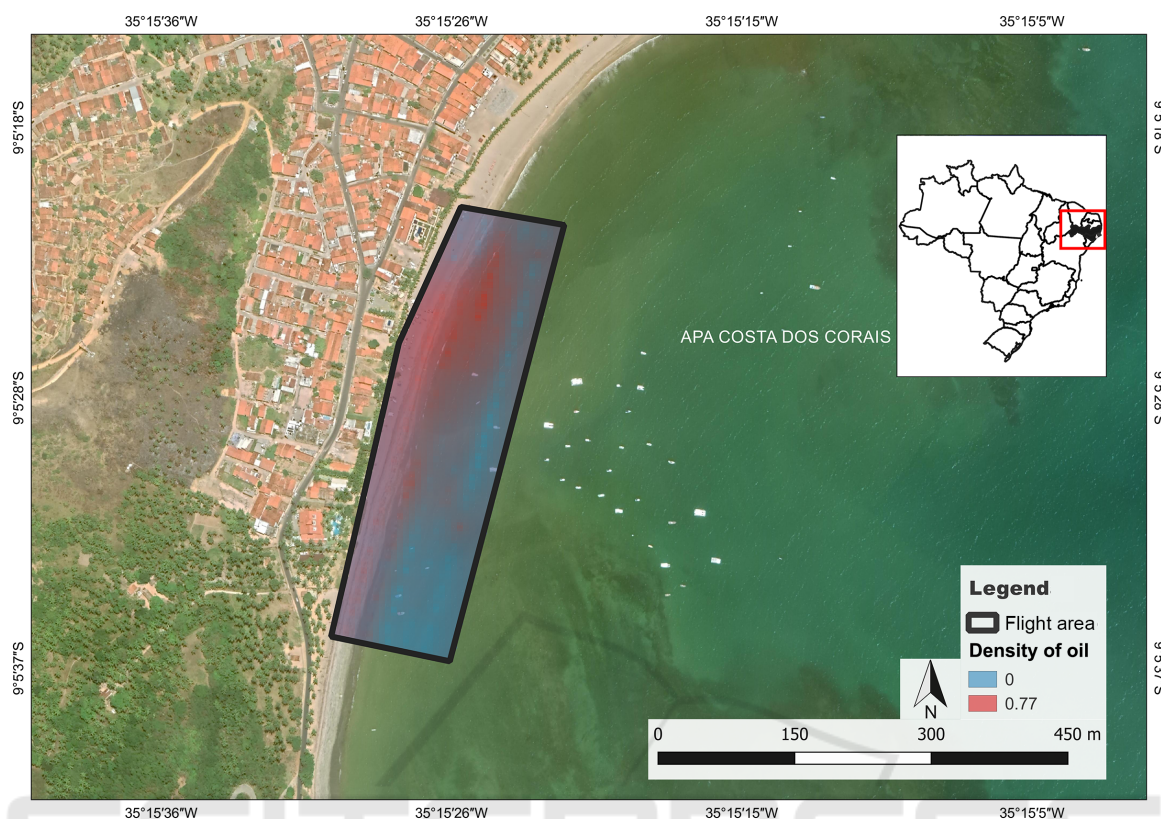
Figure 4: Visualization of the resulting heatmap built from images collected in the municipality of Japaratinga, following the pipeline shown in Figure 1. Our methodology allows to quickly identify a red spot indicating the presence of oil pollution in the beach.

(a) True negative predictions.

(b) True positive predictions.

Figure 5: Examples of correctly predicted patches of the heatmap shown in Figure 4.

environmental impacts. It is worth mentioning, however, that the trained model may not generalize to different coastal environments, requiring retraining the model.

4 CONCLUSION

In this paper, we proposed a DL approach based on low-cost UAVs images to efficiently identify and visually localize oil floating on the water surface or washing up on beaches. By combining a CNN, trained in

a supervised manner to evaluate small patches, with a geospatial visual system, we showed that oil spills can be rapidly detected and localized, allowing immediate reactions and avoiding substantial environmental impact. Our classifiers achieved up to 93.6% of accuracy and an F_1 score of 78.6% in a small dataset comprised of 6,907 patches, revealing promising results that may be enhanced in future work by exploiting larger datasets and more elaborate DL techniques, such as image segmentation networks.

ACKNOWLEDGMENT

REFERENCES

Al-Ruzouq, R., Gibril, M. B. A., Shanableh, A., Kais, A., Hamed, O., Al-Mansoori, S., and Khalil, M. A. (2020). Sensors, features, and machine learning for oil spill detection and monitoring: A review. *Remote Sensing*, 12(20):3338.

Beyer, J., Trannum, H. C., Bakke, T., Hodson, P. V., and Collier, T. K. (2016). Environmental effects of the deepwater horizon oil spill: a review. *Marine pollution bulletin*, 110(1):28–51.

Burger, J. (1997). *Oil spills*. Rutgers University Press.

Cazzato, D., Cimarelli, C., Sanchez-Lopez, J. L., Voos, H., and Leo, M. (2020). A survey of computer vision methods for 2d object detection from unmanned aerial vehicles. *Journal of Imaging*, 6(8):78.

Chollet, F. et al. (2015). Keras. https://keras.io.

Davaasuren, N., Marino, A., Boardman, C., Alparone, M., Nunziata, F., Ackermann, N., and Hajnsek, I. (2018). Detecting microplastics pollution in world oceans using sar remote sensing. In *IGARSS*, pages 938–941. IEEE.

Fingas, M. and Brown, C. E. (2018). A review of oil spill remote sensing. *Sensors*, 18(1):91.

Han, F., Shan, Y., Cekander, R., Sawhney, H. S., and Kumar, R. (2006). A two-stage approach to people and vehicle detection with hog-based svm. In *Performance Metrics for Intelligent Systems 2006 Workshop*, pages 133–140.

Jiao, Z., Jia, G., and Cai, Y. (2019). A new approach to oil spill detection that combines deep learning with un-

manned aerial vehicles. *Computers & Industrial Engineering*, 135:1300–1311.

Kingma, D. P. and Ba, J. (2014). Adam: A method for stochastic optimization. *arXiv preprint arXiv:1412.6980*.

Kingston, P. F. (2002). Long-term environmental impact of oil spills. *Spill Science & Technology Bulletin*, 7(1-2):53–61.

Kussul, N., Lavreniuk, M., Skakun, S., and Shelestov, A. (2017). Deep learning classification of land cover and crop types using remote sensing data. *IEEE Geoscience and Remote Sensing Letters*, 14(5):778–782.

Ladle, R., Malhado, A. C., Campos-Silva, J., and Pinheiro, B. (2020). Brazil's mystery oil spill: an ongoing social disaster. *Nature*, 578(7793):37–37.

Magalhães, K. M., de Souza Barros, K. V., de Lima, M. C. S., de Almeida Rocha-Barreira, C., Rosa Filho, J. S., and de Oliveira Soares, M. (2021). Oil spill+ covid-19: A disastrous year for brazilian seagrass conservation. *Science of The Total Environment*, 764:142872.

Magris, R. A. and Giarrizzo, T. (2020). Mysterious oil spill in the atlantic ocean threatens marine biodiversity and local people in brazil. *Marine pollution bulletin*, 153:110961.

Massa, L., Barbosa, A., Oliveira, K., and Vieira, T. (2021). Lrcn-retailnet: A recurrent neural network architecture for accurate people counting. *Multimedia Tools and Applications*, 80(4):5517–5537.

Miranda, R. J., Almeida, E. C., Pinto, T. K., Sampaio, C. L., Pereira, P. H., Nunes, J. A., and Ladle, R. J. (2020). Re: Oil spill disaster in brazil: impact assessment neglecting unique coral reefs. *Science*.

Nogueira, V., Oliveira, H., Silva, J. A., Vieira, T., and Oliveira, K. (2019). Retailnet: A deep learning approach for people counting and hot spots detection in retail stores. In *SIBGRAPI*, pages 155–162. IEEE.

Peterson, C. H., Rice, S. D., Short, J. W., Esler, D., Bodkin, J. L., Ballachey, B. E., and Irons, D. B. (2003). Long-term ecosystem response to the exxon valdez oil spill. *Science*, 302(5653):2082–2086.

Puttemans, S., Van Beeck, K., and Goedemé, T. (2018). Comparing boosted cascades to deep learning architectures for fast and robust coconut tree detection in aerial images. In *Proceedings of the 13th international joint conference on computer vision, imaging and computer graphics theory and applications*, volume 5, pages 230–241. SCITEPRESS.

Redmon, J., Divvala, S., Girshick, R., and Farhadi, A. (2016). You only look once: Unified, real-time object detection. In *CVPR*, pages 779–788.

Ren, S., He, K., Girshick, R., and Sun, J. (2016). Faster r-cnn: towards real-time object detection with region proposal networks. *IEEE transactions on pattern analysis and machine intelligence*, 39(6):1137–1149.

Ribeiro, L., Souza, K., Domingues, E., and Magalhães, A. S. (2021). Blue water turns black: economic impact of oil spill on tourism and fishing in brazilian northeast. *Current Issues in Tourism*, 24(8):1042–1047.

Shaban, M., Salim, R., Abu, H., Khelifi, A., Shalaby, A., El-Mashad, S., Mahmoud, A., Ghazal, M., and El-Baz, A. (2021). A deep-learning framework for the detection of oil spills from sar data. *Sensors*, 21(7):2351.

Sissini, M., Berchez, F., Hall-Spencer, J., Ghilardi-Lopes, N., Carvalho, V., Schubert, N., Koerich, G., Diaz-Pulido, G., Silva, J., et al. (2020). Brazil oil spill response: Protect rhodolith beds. *Science*, 367(6474):156–156.

Soares, M., Teixeira, C., Bezerra, L., Rossi, S., Tavares, T., and Cavalcante, R. (2020). Brazil oil spill response: Time for coordination. *Science*, 367(6474):155–155.

Vyas, G., Bhan, A., and Gupta, D. (2015). Detection of oil spills using feature extraction and threshold based segmentation techniques. In *2015 2nd International Conference on Signal Processing and Integrated Networks (SPIN)*, pages 579–583. IEEE.

Zacharias, D. C., Gama, C. M., and Fornaro, A. (2021). Mysterious oil spill on brazilian coast: Analysis and estimates. *Marine Pollution Bulletin*, 165:112125.

Zhang, Z., Liu, Q., and Wang, Y. (2018). Road extraction by deep residual u-net. *IEEE Geoscience and Remote Sensing Letters*, 15(5):749–753.